



A high-power, robust piezoelectric energy harvester for wireless sensor networks in railway applications

Guansong Shan, Dong Wang, Zheng Jun Chew, Meiling Zhu *

Faculty of Environment, Science and Economy, University of Exeter, Exeter, UK

ARTICLE INFO

Keywords:

Piezo stack energy harvesting
High-power
High durability and robustness
Frequency up-conversion mechanism
Railway track vibration
Wireless sensor networks

ABSTRACT

Piezoelectric energy harvesting techniques are increasingly seen as promising power sources for wireless sensor networks that monitor railway infrastructure. However, the piezoelectric generators currently available for railway applications suffer from low power output, as well as inadequate durability and robustness. To tackle these issues, this study introduces a novel, high-power, sturdy piezo stack energy harvester's design, optimization, and testing for powering wireless sensor networks in rail systems. The aim is to improve both the power output and the durability and robustness of the device. The proposed harvester's high-power generation is facilitated by a frequency up-conversion mechanism, mechanical transformer design and optimization, and the application of the piezo stack's compression mode (d_{33} mode). The frequency up-conversion mechanism allows the harvester to function at low-frequency track vibrations with high power. The mechanical transformer significantly magnifies the force exerted on the piezo stack. The compression mode boosts the energy conversion efficiency due to its higher coupling factor. To enhance durability and robustness, innovative approaches are employed. The mechanical transformer is optimized for maximum energy transmission efficiency without exceeding the material's fatigue limit. Moreover, the piezo stack is designed to operate under pre-compression, preventing tensile stress and taking advantage of the piezoelectric ceramics' remarkable compressive strength. Plate springs are also integrated into the mechanical transformer to maintain motion along the vibration direction. Experimental results from prototype testing provide strong evidence for the high-power output of the proposed harvester and its ability to power a wireless sensor. A maximum power of 511 mW and an average power of 24.5 mW are achieved at a harmonic excitation with 21 Hz and 0.7 RMS (Root Mean Square) g, while a maximum power of 568 mW and an average power of 7.3 mW are generated under a measured railway track vibration signal.

1. Introduction

Railway transportation systems are crucial for global economies and people's everyday lives, with over 854,000 kilometres of railway lines in use each year [1]. Wireless sensor networks (WSNs) play a crucial role in monitoring railway infrastructure, including bridges, railway tracks, track beds, and track equipment, as well as vehicle health monitoring, such as chassis, bogies, wheels, and wagons [2]. The utilization of WSNs offers numerous benefits that significantly improve railway operations, safety, and reliability. One key advantage of employing WSNs for condition monitoring is the reduction in human inspection requirements. Automated monitoring systems equipped with wireless sensors can continuously gather real-time data from various components of the railway infrastructure and vehicles. By eliminating or minimizing

manual inspections, WSNs save time and resources while ensuring a more efficient monitoring process. Moreover, WSNs help detect faults at an early stage, even before they escalate into critical issues, and thus enables proactive maintenance actions, allowing railway operators to address problems promptly and avoid costly downtime or disruptions. It also helps prevent accidents, reduce the risk of catastrophic failures, and ensure the overall safety of railway operations. While wireless sensor networks offer invaluable advantages for monitoring railway infrastructure and vehicle health, the lack of a dependable power source remains a significant challenge. Traditional power sources, such as batteries and cables, have limitations. Batteries have a restricted life-span, complicated replacement process, and negative environmental impact. Cables, on the other hand, can be challenging to install, particularly in remote areas or specific underground tunnels. These

* Corresponding author.

E-mail address: m.zhu@exeter.ac.uk (M. Zhu).

<https://doi.org/10.1016/j.sna.2023.114525>

Received 27 March 2023; Received in revised form 7 June 2023; Accepted 29 June 2023

Available online 30 June 2023

0924-4247/© 2023 The Author(s). Published by Elsevier B.V. This is an open access article under the CC BY license (<http://creativecommons.org/licenses/by/4.0/>).

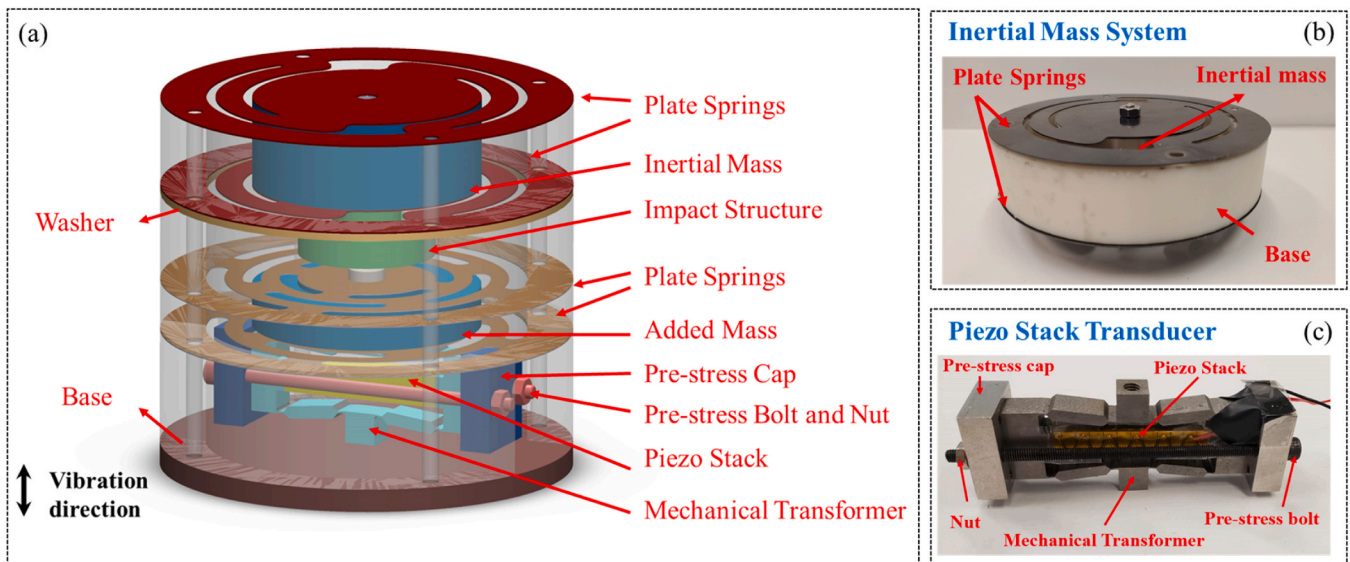


Fig. 1. (a) A schematic of the proposed energy harvester design, and detailed illustrations of (b) the inertial mass system prototype and (c) the piezo stack transducer prototype.

issues have driven researchers to investigate energy harvesting technologies, which convert ambient energy from the environment into electrical power. One potential energy source is vibrations from railway tracks. Energy can be harvested from the vertical movements of railway tracks [3], railway sleepers [4], and train bogies [5] generated by passing trains.

While electromagnetic methods have the capability to generate power in the range of hundreds of milliwatts [6] or even watts [7], their implementation in the railway metallic environment is challenging due to the involvement of a moving magnet [8] or their relatively large size, which hinders regular track maintenance [9]. In contrast, the piezoelectric vibration energy harvesting technique has emerged as a promising approach to harness power from railway track vibrations due to its simple design, ease of scalability, remarkable energy and power density, versatile applications, and customisable shapes [10–12].

Initially, one piece of piezoelectric element was bonded directly to the railway track, resulting in 0.053 mW power output on average [13]. However, the initial output was considered inadequate, prompting the creation of various designs focused on enhancing power output. One such design incorporates piezoelectric cantilevers with bending modes (d_{31} modes) as suggested in a particular reference, owing to their straightforward structures [14–17]. For instance, a piezoelectric cantilever was developed and a maximum power output of 4.9 mW was achieved during laboratory testing under conditions of 5 g and 7 Hz [15]. Li et al. [18] designed a cantilever array composed of six cantilevers to expand the frequency range of the harvester, and lab tests revealed that the average power was 200 μ W at 55–75 Hz. In addition to the cantilever structure, a drum transducer was introduced by exploiting the bending motion of the piezoelectric ceramic under concentrated force excitation [19]. According to the experimental results, a set of 16 drum transducers was capable of generating RMS power output of 102 μ W when the train was travelling at a speed of 0.5 km/h. However, the transducer needs to be installed under the sleeper, which may not be practical for real applications. To further enhance the energy harvesting performance, piezo stacks with compression modes (d_{33} modes) have been investigated taking advantage of the increased coupling factor. For instance, a piezo stack transducer operating in compression mode was introduced to harvest the railway track vibration energy and produced a mean power of 0.34 mW [20]. Nevertheless, the power output generated solely by the piezo stack remains unsatisfactory.

Generally, despite the high energy and power density potential

exhibited by piezoelectric energy harvesters, the current state-of-the-art designs and methods for using them in railway applications have relatively low levels of harvested power, ranging from a few to hundreds of microwatts. This level of power can be utilized to operate condition monitoring sensor nodes that consume low levels of power and measure low time-varying signals such as temperature and humidity [21,22]. However, these signals are often insufficient for early fault diagnosis of systems. Current condition monitoring technologies rely on fast time-varying signals such as vibration and acoustic emission [23,24], which require high sampling rates and the processing and wireless transmission of substantial amounts of raw data [25]. For instance, it has been reported that a self-powered vibration wireless sensor node has an average power consumption of around 7.2 mW [26]. Therefore, the power generated by piezoelectric railway energy harvesters needs to be enhanced.

Besides the insufficient power supply, poor durability and robustness are also hindering factors for the railway application of piezoelectric energy harvesters. The commonly used cantilever structures are not suitable for railway use because of the elevated risk of fracture when subjected to the intense acceleration caused by passing trains [27]. One of the reasons is that the large displacement of the inertial mass caused by the high acceleration can exceed the breaking stress of the cantilever at the support. Another reason is that piezoelectric ceramics in cantilever structures work in a bending mode whose strength is lower. It was reported that piezoelectric ceramics have a low tensile of around 45 MPa and bending strength of approximately 80 MPa [28] while possessing a high compressive strength of over 600 MPa [29]. Experimental results revealed that a piezoelectric bimorph cantilever displayed the emergence of line cracks after 2–3 min of vibration [30]. Furthermore, a bimorph cantilever with a 50 μ m steel passive layer was tested and cracked at 2 g acceleration [31]. Consequently, aside from the power output, the piezoelectric energy harvesters' durability and robustness need to be considered and improved for railway applications.

The modelling and two-peak frequency response characteristic of the piezo stack harvester was developed in our previous work [32,33]. However, such harvester still faces several challenges. Firstly, the power output heavily relies on the mechanical transformer's design, requiring optimization based on a new optimization function. Secondly, these harvesters may not withstand the harsh railway environment due to multi-directional and relatively high acceleration track vibrations, necessitating innovative strategies to enhance durability and robustness.

Thirdly, tests under measured railway track vibrations and evaluations for powering wireless sensors should be conducted for practical application. Consequently, this paper aims to optimize the design and harness its potential for real-world use. The proposed harvester will focus on both the power output and the durability and robustness of the device to meet the requirements of the targeted application. The energy harvester design will be optimised to achieve high energy transmission efficiency while maintaining sufficient safety capacity. Novel strategies will be implemented to ensure durability and robustness in the harsh industrial environment. In particular, the design of the piezo stack will feature pre-compression to avoid the generation of tensile stress in piezoelectric ceramics and utilise their high compressive strength. Meanwhile, plate springs will be incorporated into the mechanical transformer to maintain the motion along the vibration direction. Energy harvesting performance under both harmonic excitation and a measured railway track vibration signal will be evaluated using the optimised robust design and parameters. Experimental results demonstrate that the proposed harvester can generate an average power of tens of milliwatts, a significant power increase compared to the state-of-the-art piezoelectric harvesters' hundreds of microwatts. This harvester has the capability of powering the wireless sensor, which has been demonstrated in this study as well.

2. Overview and working principle of the energy harvester

2.1. Overview of the energy harvester

In the proposed energy harvester design, as depicted in Fig. 1(a), there are two distinct systems joined together using four screws: the inertial mass system (mass system) and the piezo stack transducer system (transducer system). To provide a comprehensive view, Fig. 1(b) and (c) present detailed illustrations of the inertial mass system and the piezo stack transducer prototype.

The mass system comprises an impact structure, two plate springs, and an inertial mass. The resonant frequency of the mass system is designed to align with the dominant frequency range of track vibration, using the frequency spectrum outlined in Reference [33]. The impact structure makes contact with the transducer system and thus enables the frequency-up conversion mechanism. The initial interval between the two systems can be adjusted using a washer.

On the other hand, the piezo stack transducer system consists of an added mass, two plate springs, a piezo stack, a mechanical transformer and pre-stress caps and bolts. The piezo stack is placed within the mechanical transformer. The impact structure applies a force to the mechanical transformer. The mechanical transformer then amplifies this force and transmits it to the piezo stack, which generates power. Two pre-stress caps are placed on either side of the mechanical transformer, which is then secured with two bolts and tightened by two bolts. In this way, static compressive stress is exerted on the piezo stack. This pre-compression technique utilises piezoelectric ceramics' high compressive strength and avoids the formation of tensile stress, which is essential for ensuring their durability. An added mass is incorporated to lower the transducer system's resonant frequency, which improves the power generation capability.

The designed plate springs in the two systems are distinct in shape and function. The plate springs utilized in the mass system are designed to have very low stiffness, which helps to maintain a low resonant frequency. These plate springs also enable the attainment of two adjacent vibration modes, which serves to broaden the frequency bandwidth. Conversely, with regard to the transducer system, the plate springs are intended to maintain the vertical oscillation of the mechanical transformer while preventing unwanted vibration, thus improving the overall robustness of the energy harvester.

The energy harvester operates based on the following working principle. When there is track vibration, the mass system resonates with the low-frequency vibrations and impacts with the transducer system.

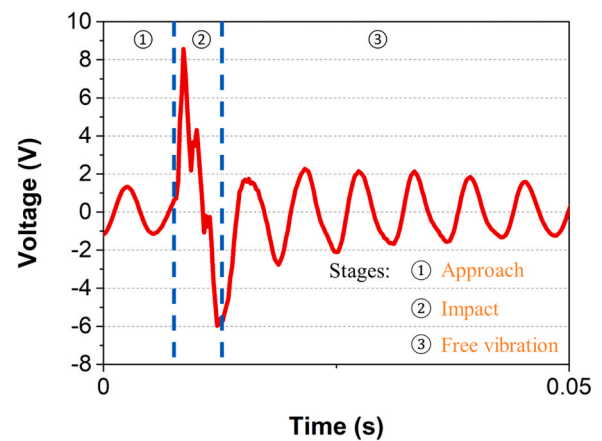


Fig. 2. Voltage output during one cycle showing the working principle of the frequency up-conversion mechanism.

This interaction leads to the generation of an impact force, which is then amplified by the mechanical transformer and subsequently transmitted to the piezo stack. As a result of this impact force, the transducer system vibrates freely at its own high resonant frequency, thereby generating electrical power.

The proposed energy harvester offers several advantages, which can be summarised as follows. Firstly, the energy harvester is capable of operating at low-frequency vibrations with high power, thanks to the frequency up-conversion mechanism. Without this mechanism, the transducer would work in an off-resonant state subjected to such low-frequency vibrations, which results in low power output due to its high stiffness. Secondly, the frequency bandwidth is broadened through the utilisation of two adjacent vibration modes of the plate springs designed for the mass system. Thirdly, the force applied to the piezo stack can be greatly amplified by the mechanical transformer, which boosts power generation. Fourthly, by employing the mechanical transformer and added mass, the stiffness of the transducer system is reduced, leading to a lower resonant frequency, which is advantageous for maximising the piezo stack's high-power generation potential. Fifthly, the piezo stack operates in the compression mode (d_{33} mode), which increases the energy conversion efficiency by 3–5 times compared to the bending mode (d_{31} mode) [34]. Finally, the stress on the piezoelectric element is uniformly distributed instead of severe stress concentration for harvesters with bending mode, leading to lower peak stress levels. Additionally, the pre-compression applied to the piezo stack by the pre-stress caps and bolts enhances the harvester's durability.

2.2. Working principle of the frequency up-conversion mechanism

The voltage output of the proposed energy harvester during one cycle is shown in Fig. 2, illustrating the three stages of the frequency up-conversion mechanism. In the first stage, the mass system begins oscillating and moves closer to the transducer system caused by the vibration of the railway tracks. In the second stage, a significant impact force is generated when the two systems collide, resulting in the maximum voltage output. During the third stage, as the mass system moves upwards, the two systems separate, and the transducer system operates in a free vibration state at its resonant frequency. This process enables the energy harvester to convert the low-frequency vibration of the railway tracks into the high resonant frequency oscillation of the piezo stack transducer, thus improving the energy harvesting performance in low frequencies. Such frequency up-conversion mechanism has also been explored in various domains, including human motion [35], ocean wave [36], bridge vibration [37], etc.

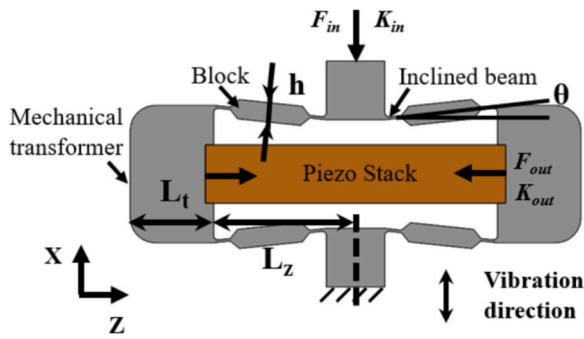


Fig. 3. The diagram of the mechanical transformer.

2.3. Working principle of the mechanical transformer

Fig. 3 illustrates the diagram of the mechanical transformer in the proposed design. The inclined beams have an angle of inclination θ . The relationship below can be established when the system is in a quasi-static state [38]:

$$F_{out} = \cot\theta F_{in} = \alpha F_{in} \quad (1)$$

$$K_{in} = \frac{\beta}{\alpha^2} K_{out} \quad (2)$$

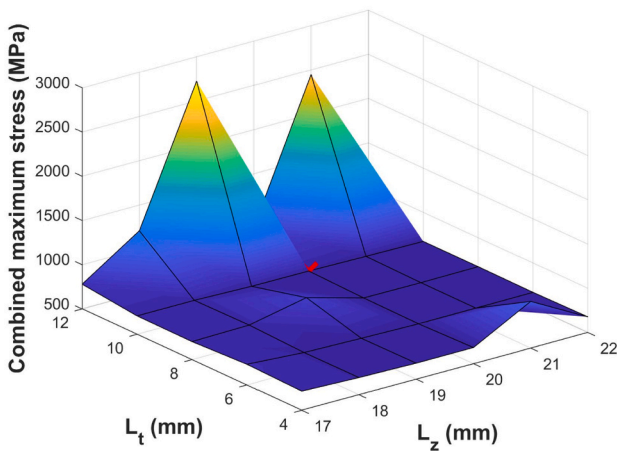
where F_{out} is the output force of the piezo stack, F_{in} is the input force of the mechanical transformer, α is the force magnification ratio of the mechanical transformer, K_{in} and K_{out} are the effective spring constants in the X and Z direction respectively, β is the energy transmission ratio of the mechanical transformer.

According to these equations, it can be inferred that the input force F_{in} is amplified by a factor of $\cot\theta$ through the force amplification mechanism of the mechanical transformer, and the stiffness is simultaneously reduced along the Z-axis, represented by K_{out} . As the electric power output is proportional to the square of the force applied to the piezo stack, the mechanical transformer leads to a considerable enhancement in power generation.

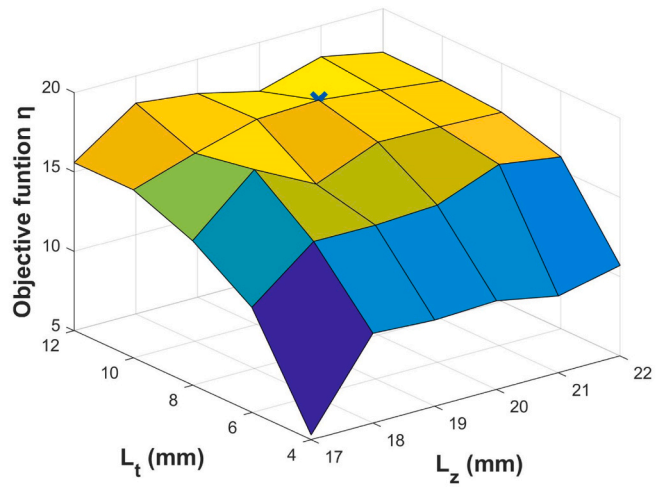
3. Design of the energy harvester

3.1. Optimisation of the mechanical transformer

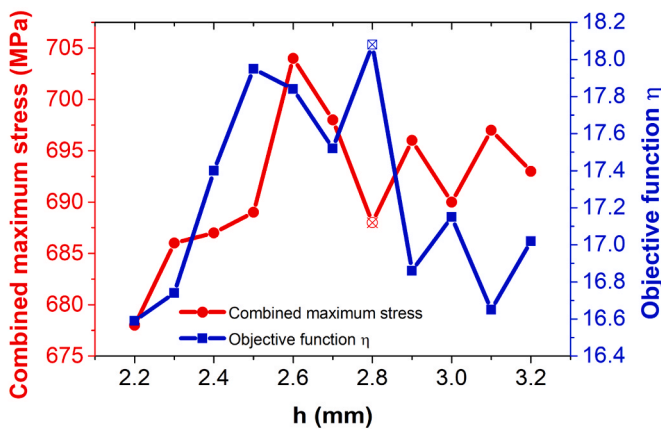
The design of the mechanical transformer is crucial for ensuring the safety and performance of the harvester, as it is the weakest component and has a crucial role in the amplifying force applied to the piezo stack. To extract more power, the mechanical transformer is expected to have



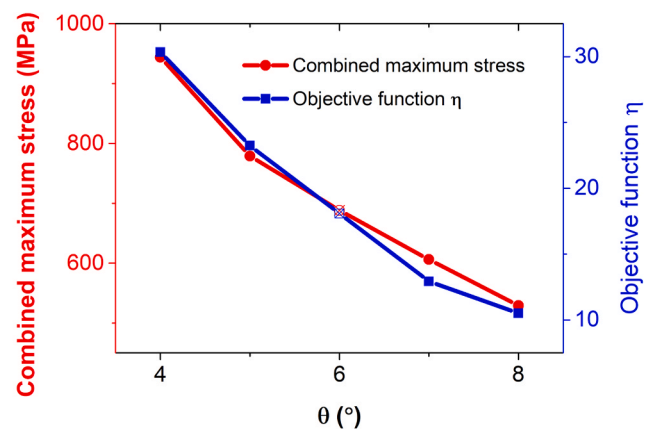
(a)



(b)



(c)



(d)

Fig. 4. The objective function and the combined maximum stress with different parameters (length L_z and thickness L_t of the transformer, block thickness h , and inclined angle θ). The optimal mechanical transformer is selected with $L_z=20$ mm, $L_t=10$ mm, $\theta=6^\circ$, and $h=2.8$ mm (represented by the symbol “x”).

both high energy transmission efficiency and adequate safety capacity. Optimizing the geometric parameters of the mechanical transformer is necessary to achieve these functions.

To enable easy bending of the beams, the inclined beams of the mechanical transformer are designed with thin ends and a thick block in the middle having a thickness of h . The thin ends act as flexure hinges, while the thick block reduces beam deformation and minimizes the storage of elastic energy. The thin ends should be as narrow as possible to achieve a high energy transmission efficiency while guaranteeing the stress demands. Consequently, the thickness of the thin ends is 0.4 mm. The geometric size of the piezo stack is $7 \times 7 \times 36$ mm. The length of the transformer L_z and the thickness of the transformer L_t determine the total length of the mechanical transformer. L_z affects the interaction between the mechanical transformer and the piezo stack, while L_t influences the deformation of the mechanical transformer. A set of parameters that define the mechanical transformer is shown in Fig. 3 and requires optimization.

The input force is magnified by the mechanical transformer, as shown in the following equation.

$$\alpha = \frac{F_{out}}{F_{in}} \quad (3)$$

The power generated in the piezo stack is proportional to the square of applied force on the stack F_{out} , and hence is proportional to the square of the force magnification ratio α [39].

Despite the force magnification, not all the energy is transferred to the piezo stack. Some of the strain energy stored in the mechanical transformer cannot be converted into electricity. Thus, the energy transmission efficiency of the mechanical transformer, denoted by β and calculated by the following equation, is also a critical factor to consider.

$$\beta = \frac{W_{out}}{W_{in}} = \frac{2F_{out}x_{out}}{F_{in}x_{in}} \quad (4)$$

where W_{out} is the output work done on the piezo stack, W_{in} is the input work of the mechanical transformer, x_{out} is the output displacement of one side of the piezo stack, x_{in} is the input displacement of the mechanical transformer. F_{out} , x_{out} , and x_{in} are derived through Solidworks simulation with a designated F_{in} value of 100 N. Subsequently, the values of α and β can be calculated.

Hence, the objective function η should be expressed as the following function [40].

$$\eta = \alpha^2 \cdot \beta \quad (5)$$

In general, to achieve a high-power output, a large force magnification ratio α is typically desired. However, it is also essential to maximize the transfer of mechanical energy to the piezo stack through the mechanical transformer. As a result, the optimisation objective function η_{opt} of designing the mechanical transformer is to obtain a maximum η , defined as Eq. (6). Additionally, the mechanical transformer used in this work is made of spring steel 60Si2CrVA with a fatigue limit of around 750 MPa [41]. To ensure the mechanical transformer has a long lifetime and high durability, the maximum stress should not exceed the material's fatigue limit σ_{max} , rather than the yield limit, as defined as Eq. (7).

$$\eta_{opt} = \max(\eta) \quad (6)$$

$$\text{Max}(\text{stress}) \leq \sigma_{max} \quad (7)$$

When subjected to railway vibration, the mechanical transformer experiences two types of forces. The first is the impact force introduced by the impact structure. The second is the inertial force produced by the track's random vibration. To analyse the maximum stress on the mechanical transformer, our developed model [33] is used to conduct stress analysis in Solidworks under both impact force and random vibration.

The worst scenario is that the stresses under both forces achieve maximum simultaneously. Therefore, the combined maximum stress is

Table 1

Comparison of the three mechanical transformers used in the research.

Design	Combined maximum stress (MPa)	Force magnification ratio α	Energy transmission efficiency β (%)	Objective function η
1[32]	745	8.96	20.34	16.33
2[33]	583	8.98	7.84	6.32
This work	688	8.83	23.19	18.08

calculated by adding the maximum stresses under both forces. The objective function and the combined maximum stress of the mechanical transformer with different parameters are shown in Fig. 4. In general, the objective function exhibits an initial increase followed by a decrease as both L_z and L_t increase. It has been found that when L_t reaches 12 mm, the combined maximum stress experiences a significant rise. Therefore, to achieve the highest objective function while ensuring that the fatigue limit is not exceeded, the optimal values of $L_z=20$ mm and $L_t=10$ mm are chosen. In terms of the block thickness h , the maximum value of the objective function is observed at $h=2.8$ mm. It should be noted that there is some fluctuation in the objective function. This behaviour arises due to the fact that as h increases, both x_{out} and x_{in} decrease, and their ratio does not follow a linear relationship. The combined maximum stress remains primarily within the range of 680–700 MPa, which is well below the fatigue limit. Furthermore, as the inclined angle θ increases, both the objective function and the combined maximum stress exhibit a decreasing trend. To ensure the attainment of the highest objective function value while staying within the fatigue limit, a value of $\theta=6^\circ$ is chosen. Based on the above analysis, the optimal mechanical transformer is selected with $L_z=20$ mm, $L_t=10$ mm, $\theta=6^\circ$, $h=2.8$ mm, represented by the symbol “ \times ” in the figure.

Table 1 provides a comparison of the three mechanical transformers used in our research. The optimised mechanical transformer design has the highest objective function with a lower combined maximum stress compared to the other designs.

3.2. Design of the plate springs in the piezo stack transducer system

The energy harvester is intended to move along the x-axis, but the multi-directional ambient vibrations and the eccentric impact between the two systems can cause multi-directional forces that could be harmful to the mechanical transformer. To examine the effects of these forces on the combined maximum stress, the impact and inertial forces are applied along the 3-axis respectively, as depicted in Fig. 5(a). The combined maximum stresses from the y-axis and z-axis are 2248 MPa and 2647 MPa, respectively, which are three to four times higher than that from the x-axis (688 MPa). This highlights the importance of ensuring that the mechanical transformer vibrates only along the x-axis during operation. Therefore, to improve stability and robustness, plate springs, as depicted in Fig. 5(b) have been designed and incorporated into the piezo stack transducer system. The connection parts in all four directions are engineered to confine vibrations along the x-axis. Employing a hollow design helps to reduce stiffness, while the central circular plate facilitates connection with the added mass. Fig. 5(c) showcases the assembly of the plate springs in the piezo stack transducer system, positioned at the top of the mechanical transformer with the added mass sandwiched in between. This arrangement effectively guides the motion of the added mass, ensuring that the mechanical transformer vibrates exclusively along the x-axis where the minimum stress is induced.

3.3. Design of the added mass

For the sake of a low height of the energy harvester and maximum utilisation of the harvester's available space, a cylindrical added mass with a diameter of up to 50 mm is implemented. However, to prevent

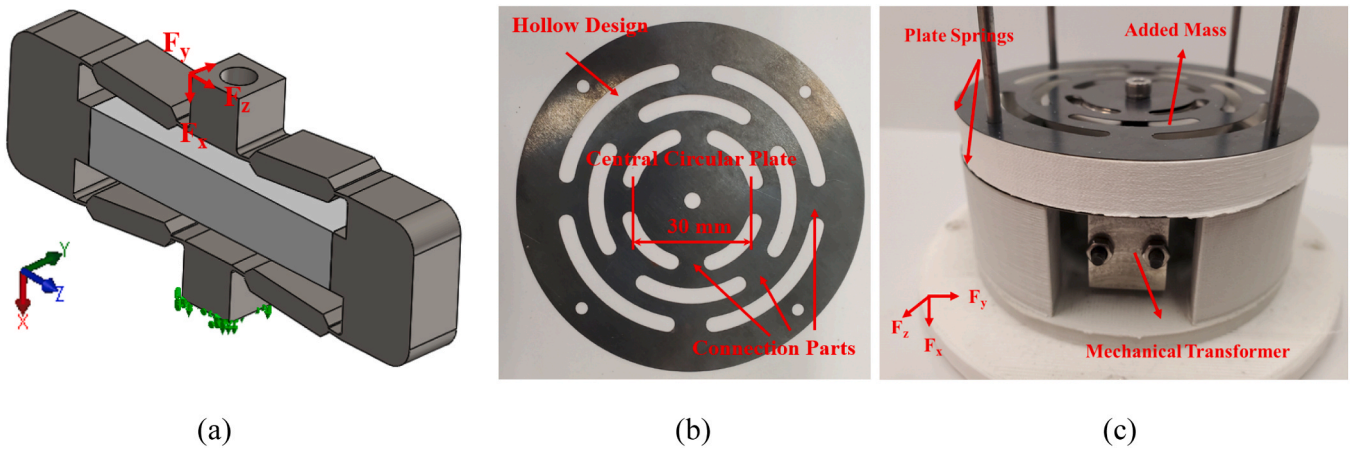


Fig. 5. (a) The model showing the impact force and the inertial force applied to the 3-axis respectively, and (b) plate springs used to support the mechanical transformer, and (c) plate springs assembled into the piezo stack transducer.

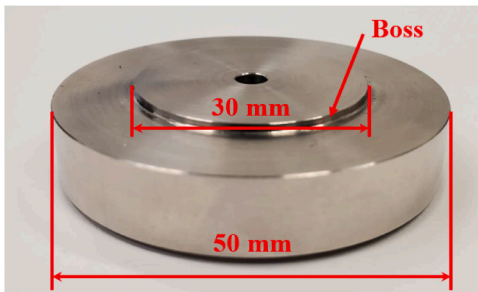


Fig. 6. Added mass in the system.

any interference with the deformation of the plate springs on the mechanical transformer, bosses with a diameter of 30 mm are strategically incorporated. These bosses are specifically designed to match the size of the central circular plate of the plate springs, allowing for a seamless integration. The design of the added mass is illustrated in Fig. 6.

4. Fabrication and experimental setup

4.1. Fabrication

To test the performance of the energy harvester, a prototype is manufactured using the optimal design. The material properties are

listed in Reference [33]. The mass system includes a 0.3 kg inertial mass, two spring steel plate springs (0.4 mm thickness), and an impact structure. The piezo stack system consists of a 0.15 kg added mass, two spring steel plate springs (0.2 mm thickness), a mechanical transformer, a piezo stack of 560 layers with d_{33} mode, and pre-stress caps and bolts. The piezo stack has a size of $7 \times 7 \times 36$ mm and is provided by Thorlabs. The mechanical transformer, made of spring steel, is assembled with an interference fit with the piezo stack. Specifically, the space on the mechanical transformer for assembling the piezo stack is machined slightly shorter than the piezo stack so that the mechanical transformer is elongated upon assembly. The assembly is then compressed by the pre-stress caps and bolts along the z-axis for reliable operation and durability of the piezo stack.

Both the top and bottom of the added mass are attached to one plate spring to allow the mechanical transformer to vibrate along the x-axis and prevent undesired vibration during operation. Washers are used to adjust the initial interval of the two systems, and the two systems are fastened together using four screws. The overall design is shown in Fig. 7 (a).

4.2. Experimental setup

Fig. 7(b) presents the experimental setup. The signal generator (Tektronix AFG3022C) and power amplifier (APS 125) are adopted to control the input signal. The energy harvester is mounted on the shaker (APS 113) and connected to a load resistor. An accelerometer is also

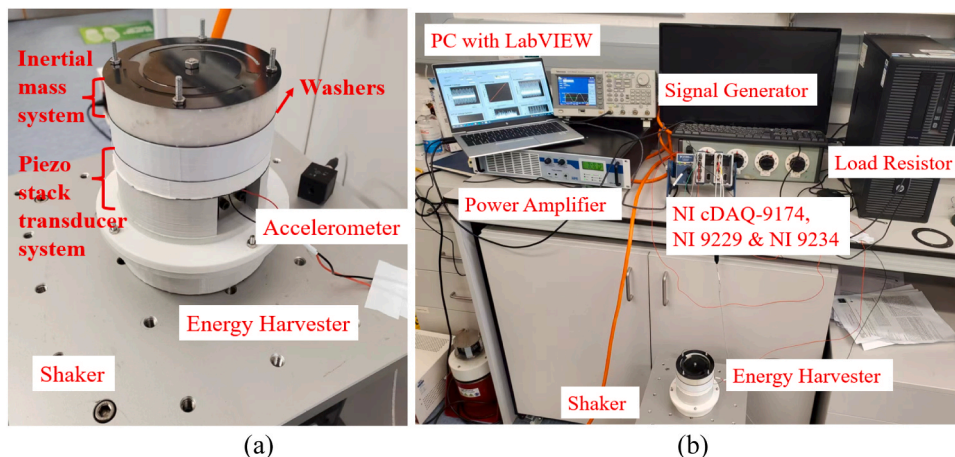


Fig. 7. (a) The prototype energy harvester, and (b) the experimental setup.

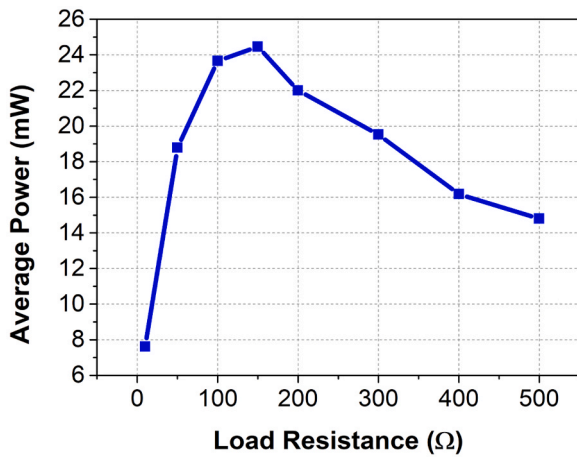


Fig. 8. The average power with regard to different load resistance with a washer of 1.6 mm actuated at 21 Hz and 0.7 RMS g.

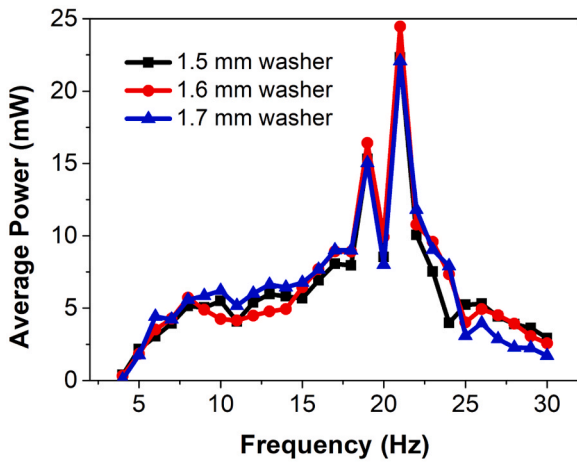


Fig. 9. The average power at different frequencies with washer thicknesses of 1.5 mm, 1.6 mm, and 1.7 mm.

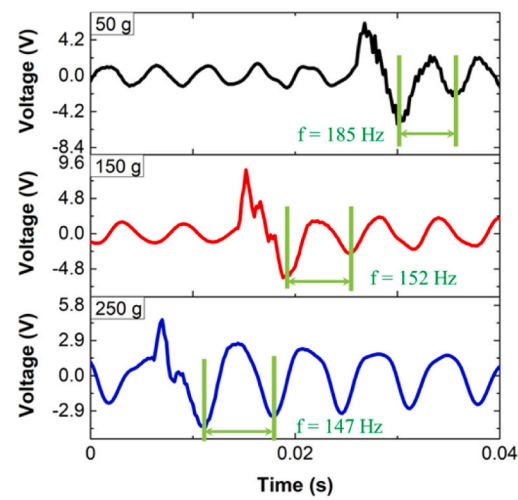
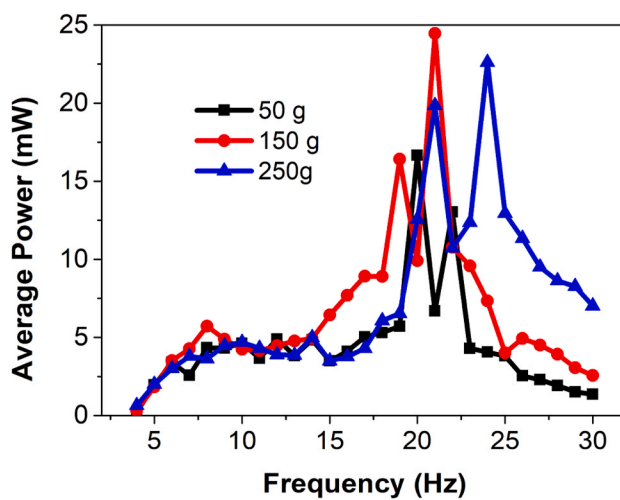


Fig. 10. (a) The average power at different frequencies with 50 g, 150 g, and 250 g added mass, and (b) their time-dependent responses showing the transducer system’s resonant frequencies.

installed on the shaker to measure the acceleration. The voltage is measured by NI cDAQ-9174 and then employed to compute the power.

5. Results and discussions

5.1. Optimisation of various parameters

5.1.1. Load resistance

Fig. 8 depicts the average power across a range of load resistance with a washer of 1.6 mm when subjected to input excitation of 21 Hz and 0.7 RMS g. The load resistance of 150 Ω is found to generate the maximum average power and is thus selected as the optimal load resistance for subsequent tests.

5.1.2. Washer

The initial interval between the two systems significantly affects the energy harvesting performance of the harvester. To achieve the desired initial interval, washers are utilized. Previous research indicates that a washer of approximately 1.5 mm thickness can generate the dual-peak frequency responses caused by the two vibration modes resulting from the plate springs on the inertial mass. Therefore, washer thicknesses of 1.5 mm, 1.6 mm, and 1.7 mm are examined at 0.7 RMS g to determine their impact on the frequency responses, as illustrated in Fig. 9.

It is found that the average power exhibits two peaks at both 19 Hz and 21 Hz, which enhances the energy harvester’s frequency bandwidth. Within the resonant region (19–21 Hz), the transducer system experiences a substantial impact force from the mass system, resulting in a significant improvement in power output. However, as the excitation frequency moves away from the resonant region, the impact force decreases, leading to reduced power output. The frequency responses across the three washer sizes (1.5 mm, 1.6 mm, and 1.7 mm) exhibit similar average power outside the resonant region. However, within the resonant region, the maximum average power is attained with a 1.6 mm washer. This configuration yields a peak average power of 24.5 mW. Consequently, a 1.6 mm washer is selected for further testing.

5.1.3. Added mass

The added mass affects both the transducer system’s resonant frequency and the maximum stress induced. Fig. 10(a) presents the frequency responses of average power with 50 g, 150 g, and 250 g added masses subjected to 0.7 RMS g acceleration, while Fig. 10(b) displays their time-dependent responses, indicating the transducer system’s resonant frequency. Results show that as the added mass increases from

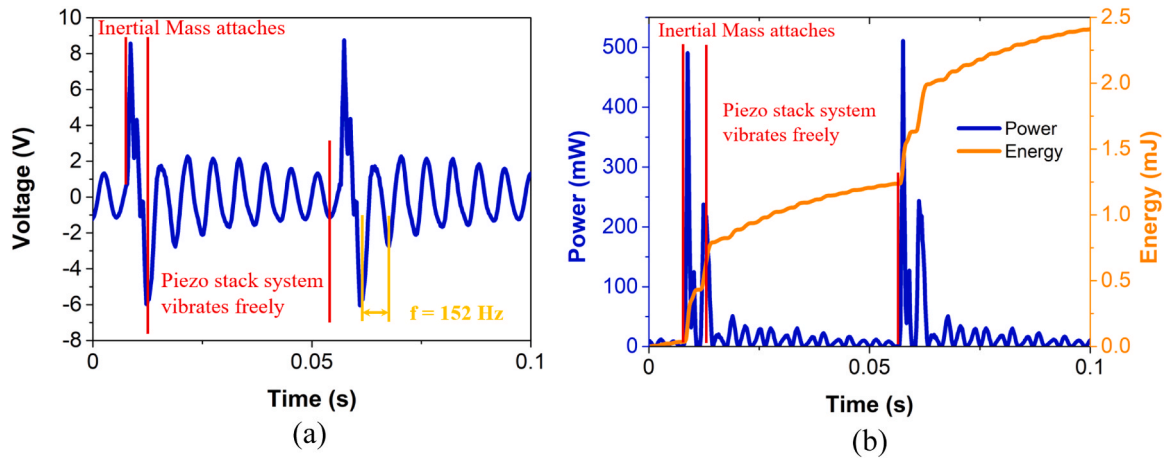


Fig. 11. Measured (a) voltage and (b) power and energy output responses in the time domain subjected to harmonic excitation.

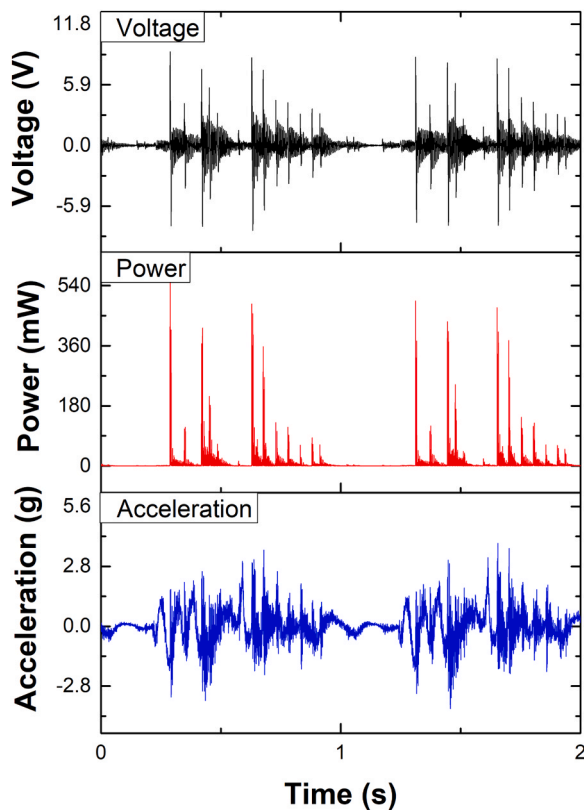


Fig. 12. Measured voltage, power, and acceleration in the time domain when actuated under a measured railway track vibration signal.

50 g to 250 g, the transducer system's resonant frequency decreases from 185 Hz to 147 Hz. Additionally, the harvester's resonant frequencies slightly shift from 20 Hz and 22–21 Hz and 24 Hz. It is because added mass influences the impact force between the two systems, allowing a minor change in the stiffness. Moreover, the maximum stress of the mechanical transformer increases with the added mass. Generally, the highest average power with 150 g and 250 g added mass are 24.5 mW and 22.6 mW respectively, while the mechanical transformer's combined maximum stresses are 688 MPa and 782 MPa. Therefore, 150 g added mass is chosen with the higher average power output and lower induced stress.

5.2. Energy harvesting performance under the optimised parameters

After investigating the effects of various parameters, an optimised design is determined with 150 Ω load resistance, a 1.6 mm washer, and 150 g added mass. The energy harvesting performance is evaluated under harmonic excitation and a measured railway track vibration signal to demonstrate the time-dependent response characteristics and the powering potentials under railway track vibration.

5.2.1. Under harmonic excitation

Fig. 11 depicts the energy harvester's voltage, power, and energy output in the time domain with a harmonic excitation of 0.7 RMS g and 21 Hz. The voltage and power responses of the energy harvester display two distinct patterns in each cycle. When the two systems collide, the voltage and power output achieve their highest levels. Conversely, upon detachment of the inertial mass system, the transducer system oscillates freely at its resonant frequency of 152 Hz, causing the voltage and power output to gradually decay under free vibration. Notably, the voltage and power output decay at a rapid pace due to the elastic energy storage from the plate springs. However, the plate springs are vital to ensure the energy harvester's durability and robustness, despite comprising voltage and power output. Overall, the proposed energy harvester converts the 21 Hz excitation into the 152 Hz free vibration of the transducer system, successfully attaining the objective of frequency up-conversion mechanism. The maximum power output is 511 mW, with an average power of 24.5 mW.

5.2.2. Under measured railway track vibration signal

In order to characterise the energy harvesting performance under railway track vibration, the input excitation is provided by a measured track vibration signal. Fig. 12 shows the measured voltage, power and acceleration (0.7 g RMS acceleration) in the time domain actuated under such a signal. The maximum power output is 568 mW with an average power of 7.3 mW. These results demonstrate that the proposed harvester performs efficiently and effectively under railway track vibration.

5.3. Tests for powering wireless sensor

The performance of the proposed energy harvester in powering a wireless sensor is assessed in the subsequent experiment. The experimental setup is presented in Fig. 13(a), where the energy harvester is connected to the energy harvesting circuit, an electrolytic capacitor (22mF), and a wireless sensor (TI SimpLink CC2650) instead of using the load resistor depicted in Fig. 7(c). The SimpLink App installed on a mobile phone is used to receive data from the wireless sensor. The

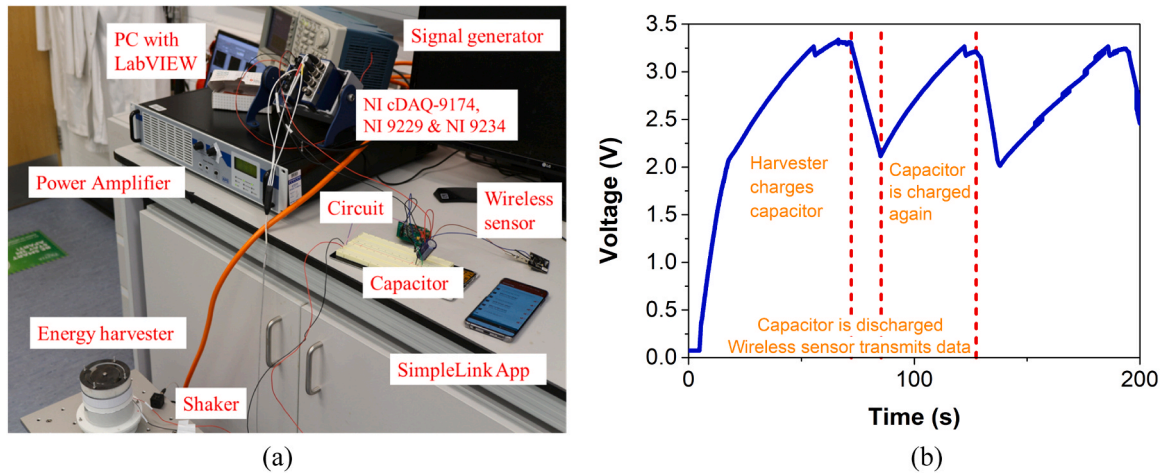


Fig. 13. Tests of the proposed energy harvester for powering wireless sensor: (a) experimental setup, and (b) voltage across the capacitor illustrating the power transfer process.

Table 2

Comparison of piezoelectric vibration harvesters for railway applications in the literature.

References	Year	Shape of Harvester	Resonant Frequency [Hz]	Installation Position	Acceleration [g]	Load Resistance [k Ω]	Power [mW]		Power Density [mW/g]
							Average	Peak	
Pasquale et al. [14]	2011	Cantilever	5.71	Bogie	1.53	210	4		0.109
Gao et al. [15]	2016	Cantilever	7	Track	5	100		4.88	< 0.081
Li et al. [18]	2014	Cantilever Array	55–75	Track	0.2	59.4	0.2	0.36	0.05
Yuan et al. [19]	2014	Plate		Sleeper	0.75 mm displacement	4000	0.1 (RMS)		
Cao et al. [20]	2022	Piezo stack	5	Track	2 mm displacement	12	0.34		
Mishra et al. [42]	2021	Cantilever	93.54	Track	0.25	5000	0.026		0.005
Dziadak et al. [43]	2022	Pendulum	14.2	Bogie	1 mm displacement	25	3.56		0.142
Cámara-Molina et al. [44]	2023	Cantilever	5.68	Bridge	1.32	33	0.38		0.003
This work		Piezo stack	19 & 21	Track	0.7 (RMS)	0.15	24.5	511	0.054

voltage across the capacitor is illustrated in Fig. 13(b) subjected to a harmonic excitation of 0.7 RMS g and 21 Hz to exhibit the power transfer process. When there is vibration excitation, the energy harvester starts converting the vibration energy into electrical energy that charges the capacitor, causing an increase in the voltage. The charging process persists until the capacitor is fully charged and reaches its maximum voltage. Subsequently, the capacitor discharges, powering the wireless sensor that transmits data to the SimpleLink App, causing the voltage to drop until it reaches the detection voltage. The capacitor then charges again, and the wireless sensor becomes inactive until the capacitor is fully charged once more, repeating the powering cycle. The results confirm that the proposed energy harvester can power a wireless sensor effectively.

5.4. Comparison with state-of-the-art literature

A comparison between the proposed vibration energy harvester and existing piezoelectric harvesters for railway applications is presented in Table 2. The results show that the proposed harvester outperforms the existing harvesters in terms of power output, generating an average power of tens of milliwatts, while the existing harvesters only produce hundreds of microwatts.

6. Conclusions

A high-power and robust piezo stack energy harvester for wireless

sensor networks in railway applications is designed, optimised, and tested in this paper. The design focuses on maximising power output, and enhancing durability and robustness. The proposed harvester's high-power production stems from the use of frequency up-conversion mechanism, the mechanical transformer design and optimisation, and the application of piezo stack's compression mode (d_{33} mode). The frequency up-conversion mechanism, realised through mechanical impact, enables the energy harvester to operate at low-frequency vibrations with high power. The impact force is then amplified by the mechanical transformer and transmitted to the piezo stack operating in d_{33} mode for a higher coupling factor. To achieve high energy transmission efficiency while ensuring longevity and durability, the mechanical transformer is optimised by maximising an objective function while keeping the maximum stress within the fatigue limit. To further enhance the durability and robustness, the piezo stack is designed in a pre-compressed state using interference fit and pre-stress caps and bolts. This prevents tensile stress and takes advantage of the piezoelectric ceramics' exceptional compressive strength. Additionally, plate springs are incorporated into the mechanical transformer to maintain its motion along the vibration direction and prevent undesired vibration, as the maximum stress from the y-axis and z-axis is significantly higher than that from the x-axis.

The performance of the harvester has been evaluated with various parameters. The harvester with optimised parameters is assessed under both harmonic excitation and measured railway track vibration signals. The proposed energy harvester successfully converts the 21 Hz

excitation into the 152 Hz free vibration of the transducer system. Under a harmonic excitation of 21 Hz and 0.7 RMS g, the harvester generates a maximum power of 511 mW with an average power of 24.5 mW. These results demonstrate that the proposed harvester can produce tens of milliwatts of power, a significant improvement over the hundreds of microwatts produced by existing piezoelectric harvesters in the literature for railway applications. Under a measured railway track vibration signal, a maximum power of 568 mW and an average power of 7.3 mW is achieved. Moreover, the harvester's capacity to power a wireless sensor is demonstrated, making it a promising power supply for wireless sensor networks in rail system.

CRedit authorship contribution statement

All authors have seen and approved the final version of the manuscript being submitted. The article is the authors' original work, hasn't received prior publication and isn't under consideration for publication elsewhere.

Declaration of Competing Interest

The authors declare that they have no known competing financial interests or personal relationships that could have appeared to influence the work reported in this paper.

Data availability

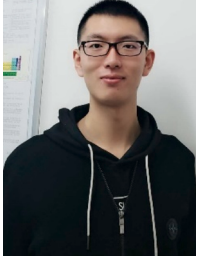
Data will be made available on request.

Acknowledgement

The authors would like to acknowledge the support of the EPSRC through the Project Zero Power, Large Area Rail Track Monitoring under Grant EP/S024840/1 and also the support of University of Exeter.

References

- [1] UIC, Railway statistics — synopsis year 2021, International Union of Railways (UIC), Paris.
- [2] V.J. Hodge, S. O'Keefe, M. Weeks, A. Moulds, Wireless sensor networks for condition monitoring in the railway industry: A survey, *IEEE Trans. Intell. Transp. Syst.* 16 (2014) 1088–1106.
- [3] X. Zhang, Z. Zhang, H. Pan, W. Salman, Y. Yuan, Y. Liu, A portable high-efficiency electromagnetic energy harvesting system using supercapacitors for renewable energy applications in railroads, *Energy Convers. Manag.* 118 (2016) 287–294.
- [4] T. Lin, J.J. Wang, L. Zuo, Efficient electromagnetic energy harvester for railroad transportation, *Mechatronics* 53 (2018) 277–286.
- [5] M. Perez, S. Chesné, C. Jean-Mistral, K. Billon, R. Augez, C. Clerc, A two degree-of-freedom linear vibration energy harvester for tram applications, *Mech. Syst. Signal Process.* 140 (2020).
- [6] M. Gao, P. Wang, Y. Cao, R. Chen, D. Cai, Design and Verification of a Rail-Borne Energy Harvester for Powering Wireless Sensor Networks in the Railway Industry, *IEEE Trans. Intell. Transp. Syst.* (2016) 1–14.
- [7] Y. Pan, T. Lin, F. Qian, C. Liu, J. Yu, J. Zuo, L. Zuo, Modeling and field-test of a compact electromagnetic energy harvester for railroad transportation, *Appl. Energy* 247 (2019) 309–321.
- [8] S. Bradai, S. Naifar, C. Viehweger, O. Kanoun, Electromagnetic vibration energy harvesting for railway applications, *MATEC Web Conf.* 148 (2018).
- [9] Y. Pan, L. Zuo, M. Ahmadian, A half-wave electromagnetic energy-harvesting tie towards safe and intelligent rail transportation, *Appl. Energy* 313 (2022), 118844.
- [10] C. Covaci, A. Gontean, Piezoelectric energy harvesting solutions: a review, *Sens. (Basel)* 20 (2020).
- [11] Z. Li, X. Peng, G. Hu, Y. Peng, Theoretical, numerical, and experimental studies of a frequency up-conversion piezoelectric energy harvester, *Int. J. Mech. Sci.* 223 (2022), 107299.
- [12] W. Liao, Y. Wen, J. Kan, X. Huang, S. Wang, Z. Li, Z. Zhang, A joint-nested structure piezoelectric energy harvester for high-performance wind-induced vibration energy harvesting, *Int. J. Mech. Sci.* 227 (2022), 107443.
- [13] C.A. Nelson, S.R. Platt, D. Albrecht, V. Kamarajugadda, M. Fateh, Power harvesting for railroad track health monitoring using piezoelectric and inductive devices, *Active and Passive Smart Structures and Integrated Systems* 2008, 2008.
- [14] G. De Pasquale, A. Somà, F. Fraccarollo, Piezoelectric energy harvesting for autonomous sensors network on safety-improved railway vehicles, *Proc. Inst. Mech. Eng., Part C: J. Mech. Eng. Sci.* 226 (2011) 1107–1117.
- [15] M.Y. Gao, P. Wang, Y. Cao, R. Chen, C. Liu, A rail-borne piezoelectric transducer for energy harvesting of railway vibration, *J. Vibroeng.* 18 (2016) 4647–4663.
- [16] A. Genovese, S. Strano, M. Terzo, Study of a Vibration-Based Piezoelectric Energy Harvester Embedded in an Air Spring, 2019 IEEE 5th International forum on Research and Technology for Society and Industry (RTSD), Florence, Italy (2019) 6.
- [17] F. Yang, M. Gao, P. Wang, J. Zuo, J. Dai, J. Cong, Efficient piezoelectric harvester for random broadband vibration of rail, *Energy* 218 (2021).
- [18] J.P. Lynch, K.-W. Wang, H. Sohn, J. Li, S. Sang, J. Tang, Implementation of a piezoelectric energy harvester in railway health monitoring, *Sensors and Smart Structures Technologies for Civil, Mechanical, and Aerospace Systems* 2014, 2014.
- [19] T. Yuan, J. Yang, R. Song, X. Liu, Vibration energy harvesting system for railroad safety based on running vehicles, *Smart Mater. Struct.* 23 (2014).
- [20] Y. Cao, R. Zong, J. Wang, H. Xiang, L. Tang, Design and performance evaluation of piezoelectric tube stack energy harvesters in railway systems, *J. Intell. Mater. Syst. Struct.* (2022), 1045389X221085654.
- [21] Y. Kuang, T. Ruan, Z.J. Chew, M. Zhu, Energy harvesting during human walking to power a wireless sensor node, *Sens. Actuators A: Phys.* 254 (2017) 69–77.
- [22] S. Roundy, P.K. Wright, A piezoelectric vibration based generator for wireless electronics, *Smart Mater. Struct.* 13 (2004) 1131.
- [23] X. Tang, X. Wang, R. Cattley, F. Gu, A.D. Ball, Energy harvesting technologies for achieving self-powered wireless sensor networks in machine condition monitoring: A review, *Sensors* 18 (2018) 4113.
- [24] M. Kande, A.J. Isaksson, R. Thottappillil, N. Taylor, Rotating electrical machine condition monitoring automation—A review, *Machines* 5 (2017) 24.
- [25] A. Stetco, F. Dinmohammadi, X. Zhao, V. Robu, D. Flynn, M. Barnes, J. Keane, G. Nenadic, Machine learning methods for wind turbine condition monitoring: A review, *Renew. Energy* 133 (2019) 620–635.
- [26] O. Rubes, J. Chalupa, F. Ksica, Z. Hadas, Development and experimental validation of self-powered wireless vibration sensor node using vibration energy harvester, *Mech. Syst. Signal Process.* 160 (2021), 107890.
- [27] M. Wischke, M. Masur, M. Kröner, P. Woias, Vibration harvesting in traffic tunnels to power wireless sensor nodes, *Smart Mater. Struct.* 20 (2011).
- [28] S. Anton, A. Erturk, D. Inman, Strength analysis of piezoceramic materials for structural considerations in energy harvesting for UAVs. *Active and Passive Smart Structures and Integrated Systems* 2010, SPIE., 2010, pp. 125–135.
- [29] Y. Kuang, Z.J. Chew, J. Dunville, J. Sibson, M. Zhu, Strongly coupled piezoelectric energy harvesters: Optimised design with over 100 mW power, high durability and robustness for self-powered condition monitoring, *Energy Convers. Manag.* 237 (2021), 114129.
- [30] H.W. Kim, A. Batra, S. Priya, K. Uchino, D. Markley, R.E. Newnham, H.F. Hofmann, Energy harvesting using a piezoelectric “cymbal” transducer in dynamic environment, *Jpn. J. Appl. Phys.* 43 (2004) 6178.
- [31] J. Palosaari, M. Leinonen, J. Juuti, H.J.M.S. Jantunen, S. Processing, The effects of substrate layer thickness on piezoelectric vibration energy harvesting with a bimorph type cantilever, 106, 2018: 114–118.
- [32] G. Shan, M. Zhu, A piezo stack energy harvester with frequency up-conversion for rail track vibration, *Mech. Syst. Signal Process.* 178 (2022), 109268.
- [33] G. Shan, Y. Kuang, M. Zhu, Design, modelling and testing of a compact piezoelectric transducer for railway track vibration energy harvesting, *Sens. Actuators A: Phys.* (2022), 113980.
- [34] T.-B. Xu, Energy harvesting using piezoelectric materials in aerospace structures. *Structural Health Monitoring (SHM) in Aerospace Structures*, Elsevier., 2016, pp. 175–212.
- [35] N. Zhou, Y. Zhang, C.R. Bowen, J. Cao, A stacked electromagnetic energy harvester with frequency up-conversion for swing motion, *Appl. Phys. Lett.* 117 (2020), 163904.
- [36] W.S. Hwang, J.H. Ahn, S.Y. Jeong, H.J. Jung, S.K. Hong, J.Y. Choi, J.Y. Cho, J. H. Kim, T.H. Sung, Design of piezoelectric ocean-wave energy harvester using sway movement, *Sens. Actuators A: Phys.* 260 (2017) 191–197.
- [37] T.V. Galchev, J. McCullagh, R.L. Peterson, K. Najafi, Harvesting traffic-induced vibrations for structural health monitoring of bridges, *J. Micromech. Microeng.* 21 (2011).
- [38] T.-B. Xu, L. Zuo, Key Issues on Flexensional Piezoelectric Energy Harvester Developments, *ASME 2019 International Design Engineering Technical Conferences and Computers and Information in Engineering Conference*, American Society of Mechanical Engineers Digital Collection, 2019.
- [39] L. Wang, S. Chen, W. Zhou, T.-B. Xu, L. Zuo, Piezoelectric vibration energy harvester with two-stage force amplification, *J. Intell. Mater. Syst. Struct.* 28 (2017) 1175–1187.
- [40] J.P. Lynch, S. Chen, L. Wang, W. Zhou, P. Musgrave, T.-B. Xu, L. Zuo, Optimal design of force magnification frame of a piezoelectric stack energy harvester, *Sensors and Smart Structures Technologies for Civil, Mechanical, and Aerospace Systems* 2015, 2015.
- [41] H. Zhao, W. Hui, Y. Nie, Y. Weng, H. Dong, Very high cycle fatigue fracture behavior of high strength spring steel 60Si2CrVA, *Chin. J. Mater. Res.* 22 (2008) 526–532.
- [42] M. Mishra, P. Mahajan, R. Garg, Piezoelectric Energy Harvesting System Using Railway Tracks. *Innovations in Electrical and Electronic Engineering*, Springer., 2021, pp. 247–259.
- [43] B. Dziadok, M. Kucharek, J. Starzyński, Powering the WSN Node for Monitoring Rail Car Parameters, Using a Piezoelectric Energy Harvester, *Energies* 15 (2022) 1641.
- [44] J. Cámara-Molina, E. Moliner, M. Martínez-Rodrigo, D. Connolly, D. Yurchenko, P. Galvín, A. Romero, 3D printed energy harvesters for railway bridges-Design optimisation, *Mech. Syst. Signal Process.* 190 (2023), 110133.



Guansong Shan received the B.Eng. and M.Eng. degrees in mechanical engineering from Jilin University, Changchun, China. He is currently working towards his Ph.D. in Energy Harvesting at the University of Exeter, Exeter, U.K. His current research focuses on piezoelectric energy harvesters for railway track vibration.



Dong Wang is a lecturer in Engineering & Entrepreneurship at University of Exeter, UK, and a research consultant at Imperial College London, UK. He received his PhD degree in Mechanical Engineering from University of Glasgow, UK. His research focuses on themes crossing over medical instrumentation, biomechanics, advanced manufacturing, energy harvesting, I4.0 technologies and technology entrepreneurship. His multidisciplinary research was developed through collaborations with consultants/surgeons, academics and industrial partners, involving developing laboratory prototypes and taking them through commercialisation, clinical validation and human testing to make a real-world impact.



Zheng Jun Chew received the B.Eng. degree in electronic and electrical engineering from the University of Strathclyde, Glasgow, U.K., in 2010 and the Ph.D. degree in electronic and electrical engineering from Swansea University, Swansea, U.K., in 2014. He was with the Energy Harvesting Research Group, University of Exeter, Exeter, U.K., in 2014, as an Associate Research Fellow. Prior to pursuing his Ph.D. degree, he was an Electrical Engineer with Sony EMCS(M) Sdn. Bhd., Malaysia, in 2010. His current research interest includes the area of power management circuits for energy-harvesting devices using novel and low-power techniques.



Meiling Zhu received the B.Eng. degree in mechanical manufacturing, the M.Eng. degree in applied mechanics, and the Ph.D. degree in mechanical dynamics all from Southeast University, Nanjing, China, in 1989, 1992, and 1994, respectively. She currently holds the Professor and the Chair in Mechanical Engineering and the Head of Energy Harvesting Research Group in the University of Exeter, Exeter, U.K. Prior to joining the University of Exeter, she was with a number of Universities: Cranfield University (2002–2013), the University of Leeds (2001–2002); Stuttgart Universität (1999–2001); the Hong Kong University of Science and Technology (1998–1999); and the Institute of Vibration Engineering Research in the Nanjing University of Aeronautics and Astronautics (1994–1998). Her current research interest includes the area of piezoelectric energy harvesting powered wireless sensor nodes for applications.